Vacuum Deposition of Thin Films of Pentaphenylcyclopentadienyl Radical and Their Electronic Properties

Sergey Lamansky and Mark E. Thompson*

Department of Chemistry, University of Southern California, Los Angeles, California 90089-0744

Received March 8, 2001. Revised Manuscript Received July 11, 2001

Thin films of 1,2,3,4,5-pentaphenylcyclopentadienyl radical ($Cp^{5\phi}$•; $\phi = C_6H_5$) were obtained upon decomposition of decaphenylplumbocene [$PbCp^{5\phi}_2$] in vacuo. Formation of the radical species was confirmed by EPR as well as electron absorption and emission spectroscopy. $Cp^{5\phi}$• decomposes slowly in solution, which is accelerated by aerobic exposure. Methods of protecting the thin films of $Cp^{5\phi}$• from aerobic decomposition were developed and used to protect the films during handling and microscopic analysis. We demonstrate that $Cp^{5\phi}$• forms amorphous thin films upon deposition, whereas thin films of the corresponding protonated compound, 1,2,3,4,5-pentaphenylcyclopentadi-2,4-ene ($Cp^{5\phi}H$), show both crystalline and amorphous structures.

1. Introduction

Significant effort has been devoted to the problem of designing molecular organic and organometallic materials with conductive or semiconducting properties.[1] Both crystalline and amorphous molecular materials have been investigated. While crystalline and polycrystalline materials typically give higher conductivities, amorphous organic molecular materials are also capable of transporting holes and electrons with reasonable carrier mobilities, making amorphous thin films useful in a wide range of applications, including xerography,[2] electroluminescent devices,[3] and thin-film transistors.[4] Amorphous materials have a significant advantage over polycrystalline ones in that they can be formed as homogeneous thin films, over large areas, on a wide variety of substrates, with no grain boundaries and very low rms roughnesses. Models have been proposed to describe the conduction process in amorphous molecular materials, which fit the experimental data fairly well.[5] Some of the best carrier mobilities in amorphous molecular solids are found for holes in arylamines.[6] Amorphous electron transporters have also been reported (e.g., metal chelates[7] and organic heterocyclic molecules),[8] but they have somewhat lower mobilities than those observed for holes in arylamines.[9]

In this report, we have examined the preparation and morphology of the films of 1,2,3,4,5-pentaphenylcyclopentadienyl radical ($Cp^{5\phi}$•). The electron in $Cp^{5\phi}$• is delocalized over the cyclopentadiene ring, giving the free radical and anionic forms of $Cp^{5\phi}$• similar structure and thus a potentially low polaron binding energy. A thin film of $Cp^{5\phi}$• forms upon thermal decomposition of its organometallic precursor $PbCp^{5\phi}_2$ under vacuum.[10] Although the Pb complex is air- and moisture-stable, $Cp^{5\phi}$• decomposes under aerobic conditions. Strategies to protect the radical from the atmosphere, for our spectroscopic measurements and for potential uses in optoelectronic devices, were developed. In this paper, we have focused on the characterization of the thin films of $Cp^{5\phi}$• both chemically, to confirm the formation of the radical, and morphologically, to predict their suitability for applications in organic thin-film devices.

2. Experimental Section

All synthetic procedures leading to decaphenylplumbocene and characterization of the products were performed according to literature procedures and are outlined in Scheme 1.[11] Chemical synthesis of $Cp^{5\phi}$• was done by oxidation of 1,2,3,4,5-pentaphenylcyclopentadi-1,3-ene lithium ($Cp^{5\phi}Li$) with silver(I) trifluoromethanesulfonate in dry tetrahydrofuran at −90 °C according to a procedure similar to the reported one.[12]

* To whom correspondence should be addressed. E-mail: met@usc.edu.

(1) *Organic Conductors*; Farges, J.-P., Ed.; Marcel Dekker: New York, 1994.

(2) *Chemistry and Technology of Printing and Imaging Systems*; Gregory, P., Ed.; Blackie Academic & Professional: London, 1996.

(3) Tang, C. W.; VanSlyke, S. A. *Appl. Phys. Lett.* **1987**, *51*, 913.

(4) Horowitz, G. *Adv. Mater.* **1998**, *10*, 365.

(5) For a theory of electronic transport in disordered solids see, for example: Bässler, H. *Phys. Status Solidi B* **1993**, *175*, 15. For an example of polaron trapping, see: Kostogloudis, G. C.; Fertis, P.; Ftikos, C. *Solid State Ionics* **1999**, *118*, 241.

(6) Koene, B. E.; Loy, D. E; Thompson, M. E. *Chem. Mater.* **1998**, *10*, 2235.

(7) (a) Kido, J.; Hayase, H.; Hongawa, K.; Okuyama, K. *Appl. Phys. Lett.* **1994**, *65*, 2124. (b) Hamada, Y.; Sano, T.; Fujita, M.; Fujii, T.; Nishio, Y.; Shibata, K. *Chem. Lett.* **1993**, 905. (c) Kido, J.; Nagai, K.; Oshashi, Y. *Chem. Lett.* **1990**, 657. (d) Nakamura, N.; Wakabayashi, S.; Miyari, K.; Fujii, T. *Chem. Lett.* **1994**, 1741. (e) Kido, J.; Endo, J. *Chem. Lett.* **1997**, 633. (f) Hamada, Y.; Sano, T.; Fujita, M.; Fujii, T.; Nishio, Y.; Shibata, K. *Jpn. J. Appl. Phys. Part 2* **1993**, *32*, L511.

(8) (a) Hamada, Y.; Adachi, C.; Tsutsui, T.; Saito, S. *Optoelectronics* **1992**, *7*, 83. (b) Kido, J. *Jpn. J. Appl. Phys. Part 2* **1993**, *32*, L917. (c) Hosokawa, C. U.S. Patent 5,142,343, 1992. (d) Sakon, Y.; Ohnuma, T.; Hashimito, M.; Saito, S.; Tsutsui, T.; Adachi, C. U.S. Patent 5,077,142, 1991. (e) Kung, T. M.; Chen, C. H. U.S. Patent 5,236,797, 1993.

(9) (a) Tokuhisa, H.; Era, M.; Tsustui, T. *Chem. Lett.* **1997**, 303. (b) Bettenhausen, J.; Strohriegl, P.; Brutting, W.; Tokuhisha, H.; Tsutsui, T. *J. Appl. Phys.* **1997**, *82*, 4957.

(10) Heeg, M.G.; Herber, R.H.; Janiak, C; Zuckerman, J. J.; Schumann, H.; Manders, W.F. *J. Organomet. Chem.* **1988**, *346*, 321.

10.1021/cm010200p CCC: $22.00
Published on Web 12/18/2001

Scheme 1. Synthetic Routes to Decaphenylplumbocene ($PbCp^{5\phi}_2$)[a]

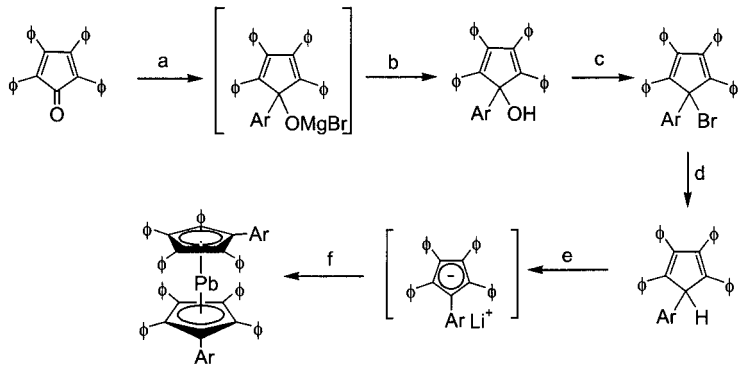

[a] a, PhMgBr, benzene, inert atm, 25 °C; b, H_2SO_4, H_2O; c, HBr, AcOH, 80 °C; d, Zn, AcOH, 100 °C; e, *n*-BuLi, THF, 0 °C, inert atm;[11] f, $PbCl_2$, THF, 0−25 °C, inert atm.[11]

Semiempirical calculations of orbital energies and absorption spectra of compounds were performed with intermediate neglect of differential overlap (INDO) method in the Cerius 3.5/ZINDO package (ZINDO = Zerner's INDO method).[13] Restricted Hartree−Fock (RHF) self-consistent field (SCF) methods were chosen for closed-shell molecules (i.e., $Cp^{5\phi}H$), and restricted open-shell Hartree−Fock (ROHF) SCF methods were chosen for open-shell molecules (i.e., $Cp^{5\phi}\bullet$). In the modeling of the absorption spectra, 15 filled and vacant orbitals were taken into consideration in configuration interaction (CI) calculations, and solvation in dichloromethane was taken into account by a self-consistent reaction field calculation (SCRF) option that is built into the ZINDO program. Geometries were preliminarily optimized with MOPAC6/AM1 method by using the BFGS optimization algorithm.

Absorption spectra were recorded on AVIV model 14DS-UV−vis−IR spectrophotometer (re-engineered Cary 14) and corrected for background due to solvent absorption. Emission spectra were recorded on PTI QuantaMaster model C-60SE spectrometer with 1527 PMT detector and corrected for detector sensitivity inhomogeneity. Emission quantum yields were determined by using Coumarin 47 as a reference. All solutions of air-stable compounds used for absorption or photoluminescence measurements were deoxygenated prior to use. The solutions of air-sensitive compounds were prepared from their thin films, protected with the thin films of material that are transparent in near-UV and visible spectral regions, with dried deoxygenated solvents by using standard Schlenk-line techniques. Mass spectra were recorded on a Hewlett-Packard 5973 Series spectrometer.

Vacuum deposition experiments were performed by using a standard high vacuum system with a background pressure of $\sim 10^{-6}$ Torr. Quartz plates (ChemGlass Inc.), silicon wafers (Recticon Corp.), or borosilicate glass−indium tin oxide plates (ITO, Delta Technologies,Ltd.) were used as substrates for deposition. ITO-coated substrates were cleaned according to the published procedure.[14,15] Copper grids for transmission electron microscopy and energy-dispersive spectroscopy (TEM/EDX) (Ted Pella, Inc.), if used as substrates for deposition, were treated with chloroform for 20 s and acetone for 5 s according to the conventional procedure of removing formovar film from the carbon-type membrane on the grid. Copper(II) phthalocyanine (CuPC) (Aldrich) used for depositions was purified by gradient sublimation prior to use. Depending on the character of the following measurement, different substrates and protective materials were used for the deposition of $Cp^{5\phi}\bullet$. For absorption, emission, and electron paramagnetic resonance (EPR) experiments on $Cp^{5\phi}\bullet$, $PbCp^{5\phi}_2$ was sublimed onto a quartz substrate in a cold sublimation finger at a vacuum of 10^{-4} to 10^{-5} Torr and a temperature of 360 °C. For EPR measurements on the solid samples, the quartz/sublimate structure was ground to a powder in the inert atmosphere. For solution EPR absorption and emission measurements, $Cp^{5\phi}\bullet$ was washed off with dry deoxygenated toluene in the Schlenk line, and the solutions were transferred to the cell or quartz tube and sealed under inert atmosphere. For TEM/EDX measurements, no protection was provided for deposited $Cp^{5\phi}\bullet$. For atomic force microscopy (AFM) and scanning electron microscopy (SEM), silicon wafers were used as substrates, and 100 Å of aluminum was deposited onto the films of air-sensitive $Cp^{5\phi}\bullet$ from V-shaped tungsten boats allowing the deposition of Al to proceed at relatively low temperatures to avoid influence of the metal on the $Cp^{5\phi}\bullet$ film morphology. The reliability of this protection method was tested on non-air-sensitive $Cp^{5\phi}H$ films, which showed the same morphology with and without Al protection. For SEM experiments, deposited structures were sputtered with gold (~100 Å).

TEM/EDX were performed on a Phillips EM420 transmission electron microscope with an acceleration voltage of 120 kV. TEM samples of air-stable $PbCp^{5\phi}_2$ were prepared by dipping the grids into a fine suspension of the complex in ethyl alcohol (Quantum Chemical Co.), which, in turn, was made by ultrasonication of the initial suspension for 10−15 min. Scanning electron micrographs were taken on a Cambridge 300 SEM with an acceleration voltage of 10 kV. Some samples for SEM were preliminarily sputtered with ~100 Å of Au. AFM images were taken on a Digital Instruments NanoScopeIII Multimode microscope in the tapping mode in ambient atmosphere.

Electrochemical measurements were performed on model 283 EG&G potentiostat/galvanostat (Princeton Applied Research). EPR spectra of the sublimed radical were taken with an X-band Bruker EMX spectrometer equipped with a standard TE102 cavity. The magnetic field was calibrated against degassed 1% perylene in sulfuric acid; a built-in frequency counter provided accurate resonant frequency values. Variable temperature experiments were performed with an Oxford (ES9000) helium cryostat. The spectra of the chemically synthesized radical at 298 K were recorded with a Bruker ER 200D-SRC spectrometer; *g* values were determined by calibration to DPPH powder.

3. Results and Discussion

3.1. Thin-Film Preparation and Characterization. Heeg et. al.[10] reported that when $MCp^{5\phi}_2$ (M = Pb, Sn, Ge) was heated, it formed the elemental metal and a purple solid that sublimed onto the cooled sublimator probe, which was assigned to $Cp^{5\phi}\bullet$. The lead

(11) Janiak, C.; Schumann, H.; Stader, C.; Wrackmeyer, B.; Zuckerman, J. J. *Chem. Ber.* **1988**, *121*, 1745.
(12) Broser, W.; Siege, P.; Kurreck, H. *Chem. Ber.* **1968**, *101*, 69.
(13) Accelrys Incorporated, San Diego, CA, http://www.accelrys.com/.
(14) Field, L. D., Ho, K. M., Lindall, C. M., Masters, A. F., Webb, A. C. *Aust J. Chem.* **1990**, *43*, 281.
(15) Shoustikov, A.; You, Y.; Burrows, P. E.; Thompson, M. E.; Forrest, S. R. *Synth. Met.* **1997**, *91*, 217.

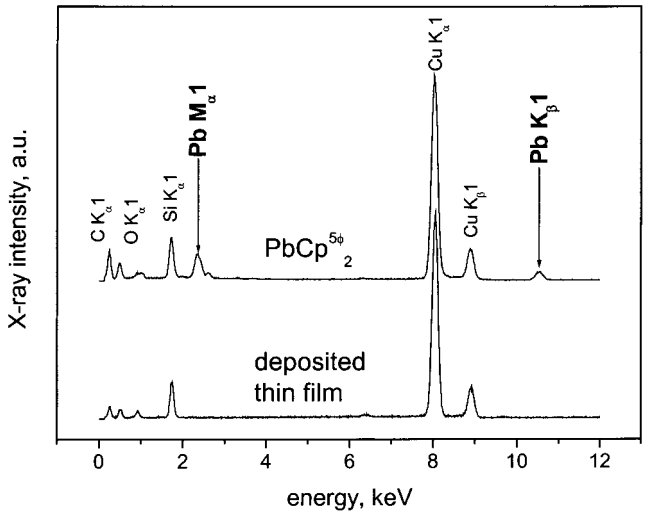

Figure 1. TEM/EDX spectra of (a) $Pb(Cp^{5\phi})_2$ complex and (b) the material deposited from the vapor upon its decomposition.

Scheme 2

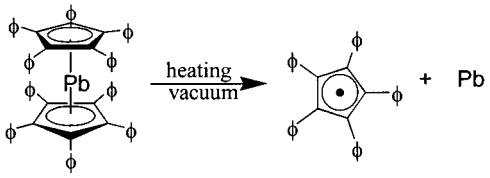

metallocene is a completely air- and water-stable compound and appears to be an ideal precursor for the air-sensitive cyclopentadienyl free radical, $Cp^{5\phi}\bullet$. Mass spectroscopy has been used to identify the major species in the gas phase formed on decomposition of $PbCp^{5\phi}_2$. Heeg et al. reported that peaks corresponding to $PbCp^{5\phi}_2{}^+$ (~1%) and $PbCp^{5\phi+}$ (100%) were both observed in the mass spectra of the decaphenylmetallocenes; however, no analysis was reported for the purple solid. In mass spectrometry analysis of $PbCp^{5\phi}_2$, we obtained a different distribution of intensities from the ions, the major ion (100%) being $Cp^{5\phi+}$ and Pb-containing species giving intensities below 4 and 1% for $MCp^{5\phi+}$ and $MCp^{5\phi}_2{}^+$ ions, respectively.

The first step in our study of films of this cyclopentadienyl radical was to verify that the product of the thermolysis of $PdCp^{5\phi}_2$ is in fact $Cp^{5\phi}\bullet$ and to determine if the purple material that is formed is contaminated with the lead metallocene. To determine if $PbCp^{5\phi}_2$ decomposes completely according to Scheme 2, i.e., there is no metal or metallocene in the deposited film, we obtained TEM energy-dispersive X-ray spectra for $PbCp^{5\phi}_2$ and the material formed upon its decomposition ($Cp^{5\phi}\bullet$ thin film). The EDX spectrum of $PbCp^{5\phi}_2$ shows X-ray peaks corresponding to carbon as well as two distinct peaks at 2.4 and 10.5 keV corresponding to the Pb $M\alpha_1$ and $L\alpha_1$ transitions, respectively (Figure 1). The deposited material shows peaks associated with carbon in its EDX spectrum but does not exhibit transitions corresponding to Pb (Figure 1). We estimate that the level of lead in this film must be less than ca. 1%, based on the ion distributions in the mass spectral data, which is the level of sensitivity of the EDX detector. This low level of lead in the film seems to be at odds with the reported mass spectral data.[10] One of the possible explanations for the observation of more lead-containing

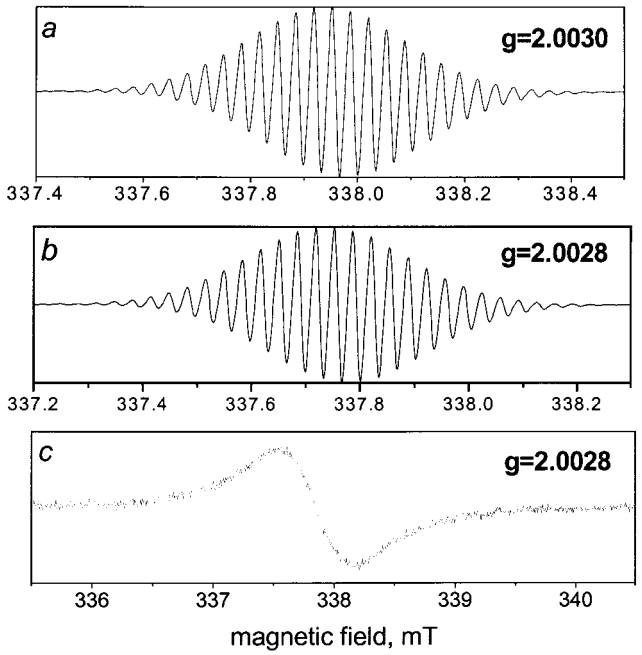

Figure 2. ESR spectra of (a) chemically prepared $Cp^{5\phi}\bullet$ in dry toluene solution and $Cp^{5\phi}\bullet$ obtained from a vacuum-deposited thin film on silica; (b) is a toluene solution of the dissolved thin film, and (c) is the solid thin film.

species in the mass spectral data is that Pb-containing compounds have ionization cross sections high enough to make them readily detectable, despite a low concentration in the gas phase. While our mass spectral analysis shows higher levels of Pb-containing species than the EDX data, our mass spectral levels are well below those reported by Heeg et al. A likely explanation of the difference is that both the mass spectral analysis and the thin-film deposition carried out in our laboratory may have been carried out at significantly lower rates of decomposition (i.e., lower temperature) than Heeg's. A high rate of decomposition of $PbCp^{5\phi}_2$ could carry the thermally unstable lead species into the vapor phase by simple mass action.

EPR measurements on chemically prepared $Cp^{5\phi}\bullet$ in dry toluene solution show a spectrum with one strong signal located at $g = 2.0030$, Figure 2a. The hyperfine structure of the spectrum is indicative of the interaction between the unpaired electron and nuclear spin magnetic moments of phenyl protons. The EPR spectrum of the deposited $Cp^{5\phi}\bullet$ is shown in parts b and c of Figure 2. This sample was prepared by heating the Pb complex to 360 °C in a glass sublimator (10^{-4} Torr) and by collecting the sublimate onto a silicate substrate. The deposited thin film was transferred into the nitrogen glovebox and dissolved with dry toluene or ground to powder together with quartz substrate to give the solid sample. The solution sample shows an EPR signal nearly identical to that of the chemically prepared $Cp^{5\phi}\bullet$ with g value of 2.0028 and identical hyperfine splitting (Figure 2b). This indicates the chemical identity of differently prepared $Cp^{5\phi}\bullet$ samples.

Despite good signal intensities, no conclusion can be made regarding the concentration of $Cp^{5\phi}\bullet$ in the vacuum-sublimed film. Several mechanisms can account for the decrease of the radical concentration with time. First, $Cp^{5\phi}\bullet$ can be deactivated by interactions with

residual oxygen in the atmosphere. Alternatively, formation of radical dimers should be considered. It is not likely for $Cp^{5\phi}$• to form dimers of the structure $C_4\phi_4C(\phi)-C(\phi)C_4\phi_4$ with a carbon−carbon bond formed directly between two cyclopentadienyl rings, due to significant steric hindrance associated with this; however, at this point, we cannot rule out a possibility of the dimerization via radical coupling through one of the phenyl groups, analogous to the process observed in the formation of dimers from Gomberg's triphenylmethyl radicals.[16]

When a solution sample of $Cp^{5\phi}$• was cooled to 60 K, the multiline signal observed at room temperature (Figure 2b) collapsed into a broadened signal with $g = 2.0028$. Under similar conditions, the spectrum of the solid $Cp^{5\phi}$• showed a slightly anisotropic EPR signal with $g = 2.0028$ and no significant line narrowing compared to the room-temperature spectra. Cooling the samples to 36 and 4 K did not lead to any spectral improvements.

3.2. Electronic Structure and Spectroscopy. More evidence of the formation of $Cp^{5\phi}$• upon decomposition of $PbCp^{5\phi}_2$ is obtained by the analysis of electronic absorption and emission characteristics of $Cp^{5\phi}$• and its closed-shell analogue $Cp^{5\phi}H$. It is useful to compare the absorption spectra of the vacuum-deposited $Cp^{5\phi}$• with spectra of chemically synthesized $Cp^{5\phi}$• and correlate them with the theoretically predicted electronic structure for the radical. The first step in this analysis is to carry out the theoretical investigation of all of the molecules to be studied. Geometries for neutral 1,2,3,4,5-penta-phenylcyclopentadi-1,3-ene ($Cp^{5\phi}H$), 1,2,3,4,5-pentaphenylcyclopentadienyl anion ($Cp^{5\phi-}$), and $Cp^{5\phi}$• were minimized, and semiempirical calculations of orbital energies and absorption spectra of compounds were performed. RHF and ROHF SCF methods were chosen for closed-shell and open-shell molecules, respectively. In the modeling of the absorption spectra, 15 filled and vacant orbitals were taken into consideration in CI calculations, and solvation in dichloromethane was taken into account by a self-consistent reaction field calculation (SCRF) option that is built into the ZINDO program. Geometry optimization of $Cp^{5\phi}$• leads to D_5 symmetry of the molecule with all torsion angles between cyclopentadienyl and phenyl rings equal to −51°, whereas $Cp^{5\phi-}$ is asymmetric (C_1 point group). In $Cp^{5\phi-}$, torsion angles between cyclopentadienyl and phenyl rings were found to be +43°, −89°, −46°, −49°, and −97° for 1-, 2-, 3-, 4-, and 5-substituted positions, respectively. An increased tendency of $Cp^{5\phi-}$ to delocalize cyclopentadienyl (Cp) ring electrons to phenyl substituents leads to observed decrease in torsion angles for three of the phenyl rings, which, in turn, is compensated by dramatic increase of torsion angles between the Cp ring and two other phenyl groups. The single-occupied highest molecular orbital of the $Cp^{5\phi}$• radical has 85% contribution from atomic functions of cyclopentadienyl core, whereas a highest occupied molecular orbital (HOMO) of the corresponding aromatic $Cp^{5\phi-}$ has 74% of such a contribution. This reflects (i) a tendency in $Cp^{5\phi-}$ to extend its aromatic structure by conjugating electrons of the Cp ring with phenyl aromatic systems and (ii) significant steric hindrance for conjugation of the phenyl rings with the Cp π system. The enhanced orbital contributions on the phenyl rings of $Cp^{5\phi-}$ could improve the electron-transfer rate to adjacent $Cp^{5\phi}$• due to good intermolecular orbital overlap. A high degree of overlap may facilitate intermolecular electron transfers, which would lead to enhanced carrier mobility.

Table 1. Calculated Absorption Spectrum Maxima of 1,2,3,4,5-Pentaphenylcyclopentadi-1,3-ene ($Cp^{5\phi}H$), 1,2,3,4,5-Pentaphenylcyclopentadienyl Anion ($Cp^{5\phi-}$), and 1,2,3,4,5-Pentaphenylcyclopentadienyl Radical ($Cp^{5\phi}$•)[a]

compd	absorption max (nm)	oscillator strength	contributing transitions
$Cp^{5\phi}H$	373	0.892	83(HOMO) → 84(LUMO)
	309	0.115	82 → 84(LUMO)
			83(HOMO) → 87
	305	0.105	83(HOMO) → 86
			83(HOMO) → 87
			83(HOMO) → 91
	301	0.233	82 → 84(LUMO)
$Cp^{5\phi-}$	375	0.209	83(HOMO) → 84(LUMO)
			83(HOMO) → 88
	362	0.688	83(HOMO) → 85
			83(HOMO) → 87
$Cp^{5\phi}$•	564	0.044	81 → 83(HOMO)
	439	0.002	81 → 85
	328	0.218	81 → 83(HOMO)
			82 → 85
	313	0.311	83(HOMO) → 85
	305	0.217	82 → 84(LUMO)

[a] Contributing transitions are marked according to numbers of molecular orbitals (MO). Designations HOMO and LUMO are used correspondingly for highest occupied MO and lowest unoccupied MO.

Theoretical predictions of the absorption spectra for $Cp^{5\phi}H$, $Cp^{5\phi-}$, and $Cp^{5\phi}$• are summarized in Table 1. In addition to absorption bands centered in the 300−370 nm region, which are typical for closed-shell $Cp^{5\phi}H$ and $Cp^{5\phi-}$ molecules ($\pi-\pi^*$ transitions; $F_{osc} \sim 0.2-0.8$), $Cp^{5\phi}$• was predicted to have absorptions at 439 and 562 nm with significantly lower intensities. This is consistent with the fact that the HOMO in $Cp^{5\phi}$• is populated with only one electron. In $Cp^{5\phi}$•, the low-energy absorption band (562 nm) corresponds to electronic transition from MO #81 (HOMO-2) to MO #83 (HOMO). The HOMO and the HOMO-1 (#82) orbitals in $Cp^{5\phi}$• are effectively degenerate, as expected from a simple Hückel analysis of the π system of Cp•.

In the measured absorption spectra, both $Cp^{5\phi}H$ and $Cp^{5\phi}$• solutions have the most intense bands centered at ca. 350 nm (Figure 3). In addition, $Cp^{5\phi}$• solution prepared from the deposited structure displays two additional bands of lower intensity at 463 and 575 nm (Figure 3). The band at 463 nm has not been previously reported.[10] Our experimental data, which is in agreement with the calculated spectra (Table 1), shows that this band is also characteristic for $Cp^{5\phi}$•.

Despite similar absorption peaks at ca. 350 nm in $Cp^{5\phi}H$ and $Cp^{5\phi}$• solutions, the emission spectra obtained from these samples on excitation at 350 nm are markedly different. The emission spectrum of neutral $Cp^{5\phi}H$ shows intense fluorescence at 454 nm, whereas emission spectrum of radical $Cp^{5\phi}$• shows a peak of comparable intensity at 390 nm under the same excitation conditions (Figure 4). Calculations show that in $Cp^{5\phi}$• and $Cp^{5\phi}H$, different transitions are active in the 320−380 nm region (Table 1). The theoretical calcula-

(16) McBride, J. M. *Tetrahedron* **1974**, *30*, 2009.

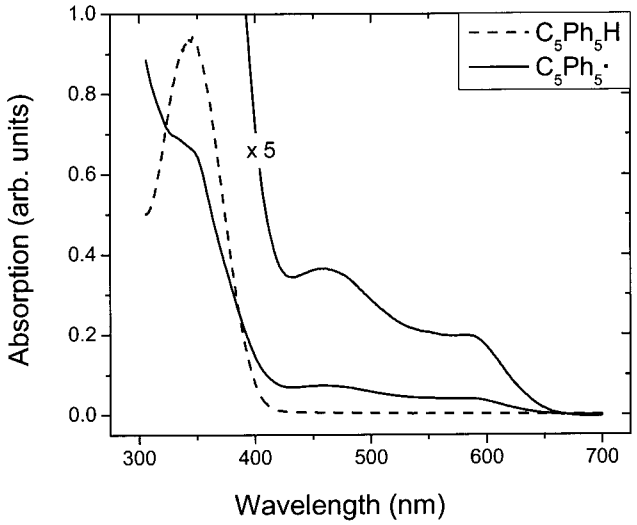

Figure 3. Absorption spectra of $Cp^{5\phi}$• in the 450−650 nm region. Inset shows full absorption spectra of $Cp^{5\phi}$• and $Cp^{5\phi}H$.

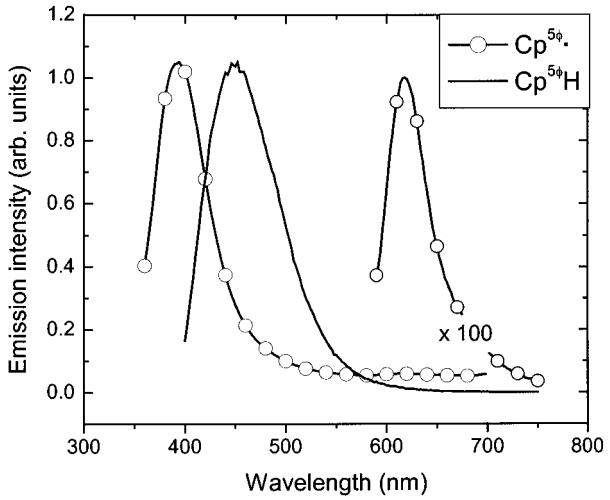

Figure 4. Normalized emission spectra of toluene solutions of $Cp^{5\phi}H$ and $Cp^{5\phi}$• (excited at 350 nm) and $Cp^{5\phi}$• (excited at 580 nm). $Cp^{5\phi}$• solution was kept in an inert atmosphere for measurements.

tions suggest that the $\pi-\pi^*$ transitions for $Cp^{5\phi}H$ should be observed at a lower energy than that for the same transition for $Cp^{5\phi}$•, which is confirmed by our observation. $Cp^{5\phi}$• also exhibits fluorescence at 610 nm when excited at 580 nm (Figure 4). Emission quantum yields were determined by literature methods[17] with the use of Coumarin 47 as a standard. The 454 nm emission of $Cp^{5\phi}H$ and the 390 nm emission of $Cp^{5\phi}$• show yields of 0.23 and 0.31, respectively (chloroform solution), whereas the 610 nm emission quantum yield was determined to be 0.002. $Cp^{5\phi}H$ shows monoexponential emission decay with the lifetime of 3.4 ns. For $Cp^{5\phi}$•, only biexponential fitting with lifetimes of 4.5 ns ($A_1 = 0.87$) and 3.0 ns ($A_2 = 0.13$) gave reliable statistical parameters. This fact may be attributed to the existence of at least two species in the $Cp^{5\phi}$• solution, which may have emissions at 390 nm upon excitation at 350 nm. One of them is thought to be $Cp^{5\phi}$• and the second one may be either an oxidized form of the radical or $Cp^{5\phi}H$.

Decomposition of $Cp^{5\phi}$• in toluene solution was accompanied by decrease in intensities of its absorption bands at 463 and 575 nm. When exposed to the atmosphere, $Cp^{5\phi}$• decomposed completely within several hours. In an inert atmosphere, decomposition was still observed but proceeded at a much slower rate (ca. 1 week). Decomposition of $Cp^{5\phi}$• in an inert atmosphere is a consequence of either a slow leak in the apparatus or a possibility of non oxidative pathways of the radical decomposition. A possible non oxidative pathway for loss of $Cp^{5\phi}$• is analogous to the process observed for Gomberg's dimer, as described above.

3.3. Topographic Characterization and Stability. Thin films of both $Cp^{5\phi}H$ and $Cp^{5\phi}$• were deposited onto different substrates under moderate vacuum of $\sim 10^{-6}$ Torr. We first examined $Cp^{5\phi}H$, because it is air stable, and felt it would be a good model for $Cp^{5\phi}$•. When deposited onto a Si wafer surface, $Cp^{5\phi}H$ formed two distinct types of structures: polycrystalline agglomerates and amorphous dots covering the Si surface very nonuniformly (Figure 5a). Over time, the amorphous regions of the film are converted into polycrystalline material. Our initial hypothesis is that $Cp^{5\phi}H$ is hydrophobic and thus does not wet the hydrophilic surface of Si sufficiently strongly to overcome the aggregation and crystallization processes. To overcome this potential problem, it was important to make the Si surface hydrophobic. This was accomplished by depositing a thin film (100−150 Å) of copper(II) phthalocyanine (CuPC), which forms a very stable and uniform film on silicon.[18] CuPC has the added benefit that it acts as a carrier injection layer for films of $Cp^{5\phi}$• in electronic and optoelectronic applications. The rms roughness for the 100 Å-thick CuPC film on Si was found to be 5.7 Å (measured by AFM), which is consistent with CuPC forming a uniform thin film. Unfortunately, $Cp^{5\phi}H$ deposited onto Si/CuPC again shows polycrystalline structures with amorphous regions uniformly surrounding the polycrystallites (parts b and c of Figure 5), which is similar to the film structure observed on the noncoated silicon substrate. The concentration and size of the crystallites were shown to depend on the deposition rate of $Cp^{5\phi}H$; i.e., the high deposition rate gives a lower degree of crystallization (parts d and e of Figure 5) The degree of crystallization in the films increased over time, as the amorphous regions gradually convert to microcrystalline material.

Films of $Cp^{5\phi}H$ were highly irregular, composed of either amorphous droplets or crystals. The structures of $Cp^{5\phi}H$ and $Cp^{5\phi}$• are different, which may lead to different thin-film morphologies for the radical, compared to $Cp^{5\phi}H$. The initial problem in exploring the morphology of the thin films of $Cp^{5\phi}$• is their air sensitivity. Since the sample is exposed to air when it is removed from the vacuum system, a protective layer must be added to prevent aerobic decomposition of the $Cp^{5\phi}$• film. The films need to be stable for at least a period of approximately 1−2 h for their morphological studies to be carried out by AFM and SEM. This protective layer must not introduce its own morphological features, since that would make AFM and SEM measurements of little use in probing the morphology

(17) Birks, J. B. *Photophysics of aromatic molecules*; Wiley-Interscience: London, 1970.

(18) Forrest, S. R. *Chem. Rev.* **1997**, *97*, 1793 and references therein.

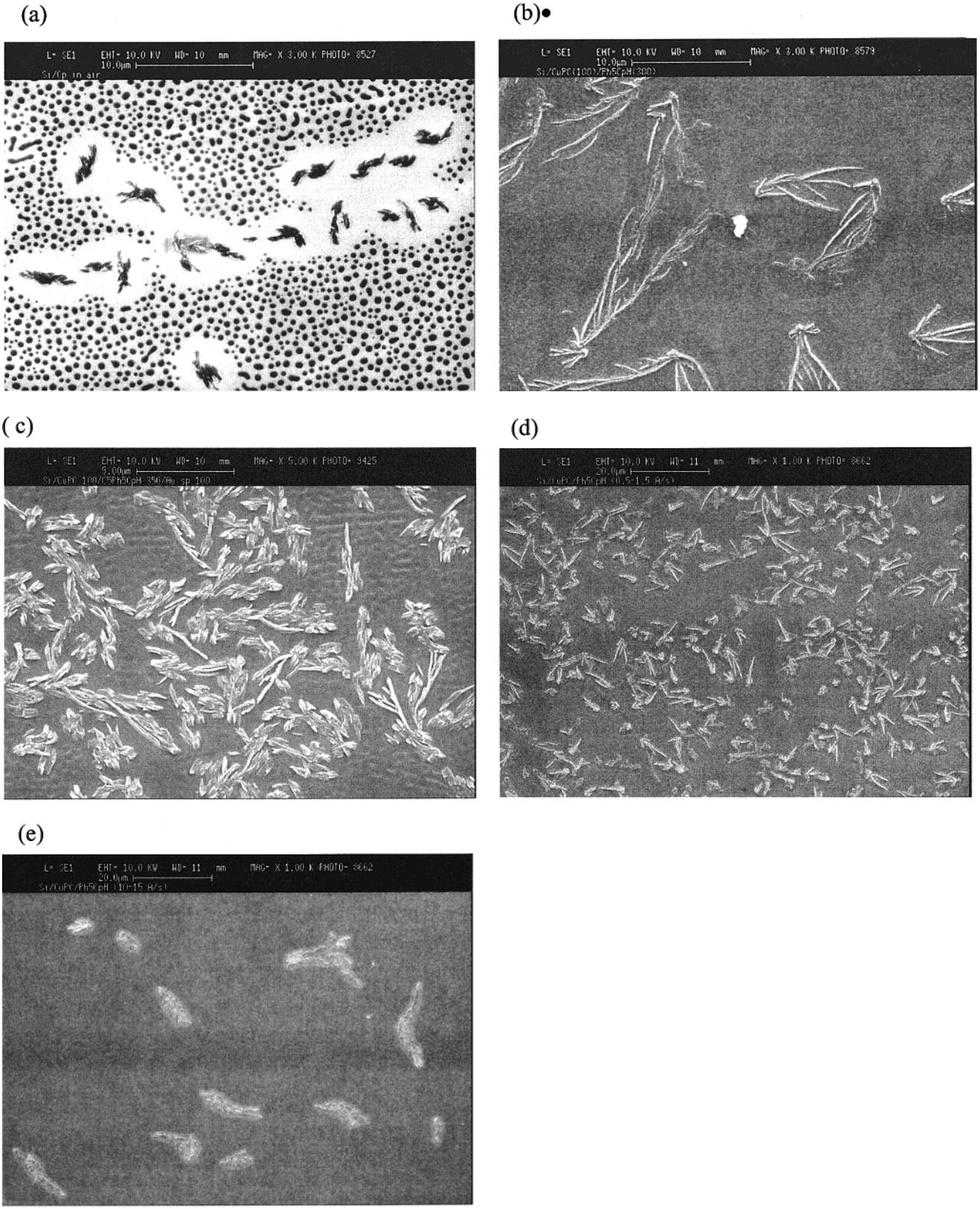

Figure 5. SEM micrograph of (a) 350 Å-thick $Cp^{5\phi}H$ film deposited onto underivatized polished Si wafer. $Cp^{5\phi}H$ builds two types of morphological structures: needle-type polycrystallites and amorphous patterns (dark spots) covering the Si surface very nonuniformly. (b) $Cp^{5\phi}H$ film deposited into the structure Si/CuPC (100 Å)/$Cp^{5\phi}H$ (350 Å). $Cp^{5\phi}H$ film amorphous areas in this sample have more uniform morphology. (c) $Cp^{5\phi}H$ film deposited into the structure Si/CuPc (100 Å)/$Cp^{5\phi}H$ (350 Å)/Al (100 Å)/$Au_{sputtered}$ (∼100 Å). (d) $Cp^{5\phi}H$ film deposited into the structure Si/CuPC (100 Å)/$Cp^{5\phi}H$ (350 Å) (deposition rate ca. 1 Å/s). (e) $Cp^{5\phi}H$ film deposited into the structure Si/CuPC (100 Å)/$Cp^{5\phi}H$ (350 Å) (deposition rate ca. 12 Å/s).

of the $Cp^{5\phi}$• film. For electron microscopy experiments, a 100 Å-thick film of Al was used to protect the $Cp^{5\phi}$• thin films. Prior to the collection of SEM images, 100 Å of Au was sputtered onto the Al-coated samples. Al was

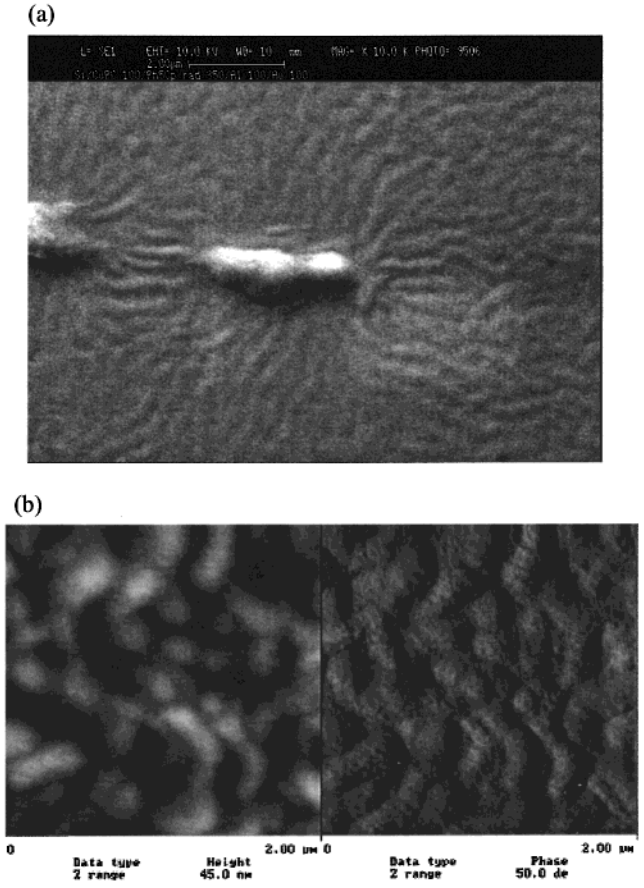

Figure 6. Thin films of $Cp^{5\phi}$• prepared in the structure Si/CuPc (100 Å)/$Cp^{5\phi}$• (350 Å)/Al (100 Å)/Au sputtered (~100 Å): (a) scanning electron microscopic image and (b) atomic force microscopic image. Both topographic and phase images are shown.

chosen because its sublimation temperature is lower than those of other applicable metals (e.g., Ag or Au), leading to less heating of the sample on applying the metal coating. The high conductivities and higher secondary electron emission coefficients of Al and Au relative to the organic films provide the added benefit of improvement in the resolution of the SEM images for these coated films when compared to the images of the uncoated $Cp^{5\phi}$• or $Cp^{5\phi}H$ films. Deposition of $Cp^{5\phi}$• onto untreated (hydrophilic) silicon leads to a globular amorphous film, consistent with poor wetting of the surface by the $Cp^{5\phi}$• film. In contrast to the films of $Cp^{5\phi}H$, the SEM images of these films did not display any crystalline features. When $Cp^{5\phi}$• was deposited onto a CuPC-coated silicon substrate and covered with protective Al film, a uniform thin film is observed, Figure 6a. In contrast to the $Cp^{5\phi}H$ films, the radical species uniformly coats the CuPC-coated substrate (i.e., no globular structures are observed). When the $Cp^{5\phi}$• film was deposited onto the coated substrate and removed from the vacuum system without the Al protection layer, crystallites were observed in the film, presumably due to crystallization of the species formed on decomposition of $Cp^{5\phi}$• in air. Thin films of $Cp^{5\phi}$• deposited at different rates (2.5, 8, and 16 Å/s) did not exhibit any differences in their morphologies. AFM images of $Cp^{5\phi}$• thin films (100 Å) deposited onto Si/CuPC (100 Å) structure and covered with Al (100 Å) are shown in Figure 6b. The images are consistent with the SEM results obtained on the same thin-film structure. The average image roughness (rms) was found to be 25 Å for the 350 Å-thick film, which is slightly larger than the corresponding value we found for a 350 Å-thick film of conventional amorphous electron-transporting material Alq_3 (18 Å) deposited onto the same substrate.

4. Summary

The 1,2,3,4,5-pentaphenylcyclopentadienyl radical ($Cp^{5\phi}$•) is formed upon the decomposition of decaphenylplumbocene $PbCp^{5\phi}_2$ in a vacuum deposition process with a very low concentration of Pb-containing species as determined by EDX spectroscopy. Also, EPR and optical spectra of the deposited film match those of chemically synthesized $Cp^{5\phi}$• confirming the formation of the $Cp^{5\phi}$• radical in $PbCp^{5\phi}_2$ vacuum decomposition. Experimental absorption spectra are in reasonable agreement with the CI spectra calculations.

$Cp^{5\phi}$• forms very uniform amorphous thin films on hydrophobic surfaces and very nonuniform films on hydrophilic surfaces. $Cp^{5\phi}H$ forms irregular films on both hydrophobic and hydrophilic surfaces, characterized by the formation of both crystalline and amorphous regions. We recently prepared substituted pentaarylcyclopentadienes ($C_5\phi_4ArH$, Ar = alkyl substituted phenyl) and their complexes with Pb, of a general formula $PbCp^{Ar4\phi}_2$, and are investigating their radical and film-forming properties. Preliminary data suggests that the lead complexes decompose in a manner directly analogous to $PbCp^{5\phi}_2$ and that the substituted derivatives form much more stable amorphous glass structures than $Cp^{5\phi}$•. We are currently studying electrical properties of thin films of $Cp^{5\phi}$• and the substituted analogues and will report that work at a later time.

Acknowledgment. We wish to thank Dr. Daniel Bolskar and Dr. Angelo DiBilio for their help with EPR measurements, Dr. Alexandre Doukutchaev for his assistance with TEM/EDX experiments, and Dr. John Worral for his valuable advice on some problems in performing SEM experiments. We are thankful to the Universal Display Corporation and the National Science Foundation for financial support of this work.

CM010200P